AIAA JOURNAL
Vol. 44, No. 4, April 2006

Formation of Secondary Vortices in Turbulent Square-Duct Flow

Alessandro Bottaro* and Houssam Soueid†
Universitá di Genova, 16145 Genoa, Italy
and
Bernardo Galletti‡
Politecnico di Torino, 10129 Turin, Italy

A linear approach, inspired by hydrodynamic stability theory, is used to describe the formation of large-scale coherent vortices for the turbulent flow that develops in a duct of square cross section. A set of equations for small-amplitude coherent motion is derived and closed with a simple mixing-length strategy. The initial condition that maximizes a chosen functional (related to either the kinetic energy of the coherent motion or the rate of turbulence production) is found through a direct/adjoint numerical approach borrowed from optimal control theory. It is found that different kinds of secondary flows can appear in the duct cross section, sustained by the mean shear. Some of these optimal states display a symmetry about the bisectors and the diagonals of the duct, in agreement with experimental observations and direct numerical simulations.

Nomenclature

E_0	=	initial energy
h	=	half-length of the duct wall along y or z
$\mathcal{I}$	=	norm of the coherent motion
$\mathcal{J}$	=	cost functional
L	=	optimization distance along x
$\mathcal{L}$	=	extended cost functional
l_m	=	mixing length
M	=	total number of interior nodes in the cross-section, $M = (N-2) \times (N-2)$
N	=	number of Gauss–Lobatto grid points along the cross-stream directions
N_L	=	number of grid points in the streamwise direction
P_T	=	turbulent pressure
$\boldsymbol{p}, \boldsymbol{u}, \boldsymbol{v}, \boldsymbol{w}$	=	vectors composing $\boldsymbol{q}$
$\boldsymbol{Q}, \boldsymbol{R}, \boldsymbol{G}_1, \boldsymbol{G}_2$	=	discretization matrices
$\boldsymbol{q}, \boldsymbol{r}$	=	vectors of direct and adjoint coherent fields
Re	=	Reynolds number, $Re = U_0 h/\nu$
S_{ij}, s'_{ij}	=	mean and fluctuating strain rates
t	=	time
U, P^*	=	base unidirectional velocity and corresponding pressure
U_0	=	peak speed in the duct
u', v', w', p'	=	fluctuating velocity components and pressure
$\tilde{u}, \tilde{v}, \tilde{w}, \tilde{p}$	=	coherent velocity components and pressure
x, y, z	=	axes along the streamwise and the cross-stream directions
α_1, α_2	=	parameters in the cost functional
Δx	=	streamwise grid spacing
δ_{ij}	=	Kronecker delta
ϵ	=	order of magnitude of the coherent variables, $\epsilon \ll 1$
λ_0	=	scalar Lagrange multiplier
ν	=	kinematic viscosity
ν_t	=	eddy viscosity
$\hat{\nu}_t$	=	dimensionless eddy viscosity, $\hat{\nu}_t = \nu_t/\nu$
ρ	=	density
Φ_v, ϕ_v	=	mean and turbulent dissipation functions
$\tilde{\omega}$	=	coherent streamwise vorticity component

Subscripts

i, j	=	variable number or cross-stream grid index
n	=	streamwise discretization index
x, y, z	=	partial derivative

Superscripts

$\overline{}$	=	time average
$\tilde{}$	=	coherent variable
$'$	=	fluctuating variable

Received 22 April 2005; presented as Paper 2005-5309 at the AIAA 4th Theoretical Fluid Mechanics Meeting, Toronto, ON, Canada, 6–9 June 2005; revision received 15 September 2005; accepted for publication 18 October 2005.

*Professor, Dipartimento di Ingegneria Ambientale, Via Montallegro 1. Member AIAA.
†Ph.D. Student, Dipartimento di Ingegneria Ambientale.
‡Postdoctoral Researcher, Dipartimento di Ingegneria Aerospaziale, Corso Duca degli Abruzzi 24.

I. Introduction

THE problem of secondary flows developing under transitional and turbulent conditions in ducts of triangular and rectangular cross section has attracted much attention after the initial observation by Nikuradse[1] that large-scale secondary motions significantly alter the mean velocity contours in the cross section of the duct. The problem has been studied from many points of view, through experiments (e.g., Brundett and Baines[2] and Gessner[3]), simulations of the Reynolds-averaged equations (e.g., Demuren and Rodi[4]), large-eddy simulations (e.g., Madabhushi and Vanka[5]), and direct numerical simulations (e.g., Gavrilakis[6]). The picture that emerges from these studies is that, from averaging over time and/or streamwise distance, a coherent motion of small amplitude exists, formed by eight vortices of very weak streamwise vorticity ω in the (y, z) cross section, symmetric about the duct diagonals and the bisection lines. Such vortices differ from those usually observed near walls in turbulent boundary layers, because they are large-scale and are locked near the corners by the imposed geometric constraints.

Conventional wisdom[7] attributes these secondary vortices to an imbalance of transverse Reynolds-normal stresses, with the term $P_2 = (\overline{v'v'} - \overline{w'w'})_{yz}$ acting as the main production term for the streamwise vorticity equation (under the assumption of fully developed flow). Hence, anisotropic turbulence models have been advocated as indispensable[8] to capture numerically secondary currents of Prandtl's second kind in the proximity of corners. On the other hand, if the assumption of fully developed flow is relaxed, other growth mechanisms for secondary structures can be invoked. In fact, in such a case ω can be produced also through the skewing of the mean shear through the source term $P_1 = U_z V_x - U_y W_x$, with U,

V, and W representing the mean flow. These issues will be further elaborated upon in Sec. V.C.

The problem of organized structures in turbulence has witnessed a rekindling of attention in the past few years because of the discovery of so-called "exact coherent states" in a number of simple wall-bounded shear flows[9–11] and the very recent experimental observation of three-dimensional traveling waves in pipe flow[12] that match quite closely the theoretically predicted states.[13,14] If transitional and turbulent shear flows can indeed be described by a small number of periodic orbits in phase space around which the dynamical system wanders for a while, before occasional escapes (escapes characterized by strong intermittent turbulent activity such as bursting events; see Kawahara and Kida[15] for the case of plane Couette flow), the consequences for statistical analysis and the control of turbulence can be far-reaching. In particular, well-defined global averages, such as the rate of energy dissipation or skin friction coefficients, could be obtained in finite time by replacing the turbulent attractor with representative periodic trajectories, thus ruling out fluctuations engendered by finite sampling. Furthermore, the crucial task of system identification for the purpose of feedback control could be greatly alleviated if a small set of unstable recurrent patterns were all that was required to develop acceptable system reconstruction capabilities. Finally, optimal control laws targeting specific patterns could be precomputed and fed dynamically to the controller as soon as flow sensors gave indications of specific occurrences.

This paper aims at making progress toward the objective of identifying organized flow states likely to appear when a fluid moves turbulently through a square duct and at providing tentative explanations for their origin. Rather than focusing on a mechanism for the creation of streamwise vorticity based exclusively on the effect of turbulence, the mechanism that is necessarily responsible for the creation of ω when the flow is considered invariant in the streamwise direction x, we assume that the turbulent flow in a square duct is streamwise inhomogeneous and, thus, we aim at modeling the initial stages of a phenomenon that is dominated by transients. Recently, Galletti and Bottaro[16] have employed a linear theory to show that the mean shear can sustain the transient amplification of cross-stream structures of large scale in square and rectangular ducts. Here, their optimization approach is further elaborated and extended, also guided by the conjecture, first outlined by Malkus,[17] that there exists a functional that turbulent shear flows tend to maximize.

II. Decomposition of the Flow and the Equations

We consider the turbulent flow in the duct sketched in Fig. 1, with cross-sectional aspect ratio $A = 1$. Our interest lies in describing the formation of secondary (corner) vortices, and in particular in assessing whether they could arise from a linear, transient amplification of large-scale, steady disturbances growing on top of a unidirectional base motion (with a turbulencelike profile). The chosen perspective is thus radically different from that of most previous studies of corner vortices,[2–4,7,8,18] which focused on fully developed states and searched for Reynolds-stress-related source terms in the kinetic energy and/or streamwise vorticity equations, capable of generating secondary currents. Our conjecture is that turbulence is a process characterized by a succession of transient events, which contribute to the creation of secondary structures through the transfer of energy between the mean, unidirectional flow and the coherent field. Although our linearized approach is clearly incapable of providing a complete description of the full energy-transfer phenomenon, and in particular of how the energy cascades from the large- to the small-scale eddies of the turbulence, it is aimed at modeling at least the initial stages of the transients alluded to earlier, with the objective of inferring a relationship between the secondary flows captured by direct numerical simulations (for example) and the coherent fields computed here.

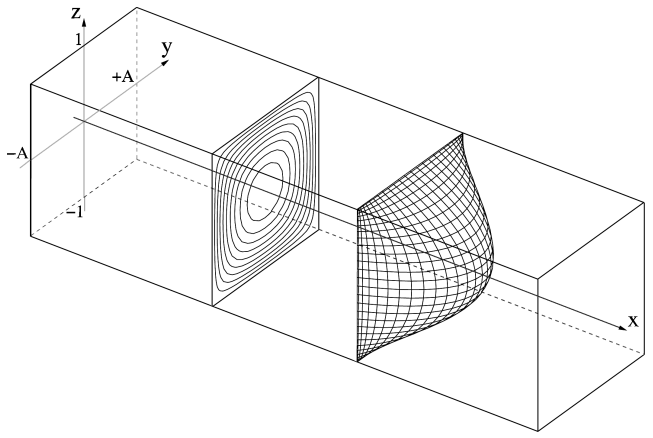

Fig. 1 Sketch of the configuration studied. Cross-stream axes have already been normalized by half-channel height h.

The approach is inspired by that of Reynolds and Hussain,[19] recently adopted and extended by Reau and Tumin[20,21] and Lifshitz et al.,[22] and it starts from a triple decomposition of the state variables as follows:

$$(u, v, w, p) = [U(y, z), 0, 0, P(x)] + [\tilde{u}(x, y, z), \tilde{v}(x, y, z), \tilde{w}(x, y, z), \tilde{p}(x, y, z)] + [u', v', w', p'](x, y, z, t)$$

The first two terms of the decomposition represent the mean, steady flow that we wish to model: the first term comprises the steady, fully developed streamwise flow $U(y, z)$, driven by the mean pressure gradient $\mathrm{d}P/\mathrm{d}x$, whereas the second one, $(\tilde{u}, \tilde{v}, \tilde{w}, \tilde{p})$, represents the x-dependent, large-scale, secondary flows. Finally, the last term (u', v', w', p') models the turbulent fluctuations. We further assume that the coherent motion (expressed by quantities with tildes) is of amplitude much smaller than either the amplitude of $[U(y, z), 0, 0, P(x)]$ or that of fluctuating quantities, so that in the equations for coherent motion, quadratic terms in $\tilde{u}_i\tilde{u}_j$ can be neglected.

Upon insertion of the triple decomposition into the equations and averaging over time (this operation is denoted by overbars), the linearized Reynolds-averaged equations are found:

$$\tilde{u}_x + \tilde{v}_y + \tilde{w}_z = 0$$

$$U\tilde{u}_x + \tilde{v}U_y + \tilde{w}U_z = -\frac{1}{\rho}\frac{\mathrm{d}P}{\mathrm{d}x} - \frac{1}{\rho}\tilde{p}_x + \nu(U_{yy} + U_{zz} + \tilde{u}_{xx} + \tilde{u}_{yy} + \tilde{u}_{zz}) - (\overline{u'u'})_x - (\overline{u'v'})_y - (\overline{u'w'})_z$$

$$U\tilde{v}_x = -\frac{1}{\rho}\tilde{p}_y + \nu(\tilde{v}_{xx} + \tilde{v}_{yy} + \tilde{v}_{zz}) - (\overline{v'u'})_x - (\overline{v'v'})_y - (\overline{v'w'})_z$$

$$U\tilde{w}_x = -\frac{1}{\rho}\tilde{p}_z + \nu(\tilde{w}_{xx} + \tilde{w}_{yy} + \tilde{w}_{zz}) - (\overline{w'u'})_x - (\overline{w'v'})_y - (\overline{w'w'})_z \quad (1)$$

with ρ the fluid density and ν the fluid kinematic viscosity.

A Boussinesq hypothesis is employed for the Reynolds stresses, with the eddy viscosity ν_t split into two parts like the mean flow $(U + \tilde{u}, \tilde{v}, \tilde{w})$, $\overline{\nu_t}$ of order one and $\tilde{\nu}_t$ "small":

$$-\overline{u_i'u_j'} = -\frac{P_T}{\rho}\delta_{ij} + (\overline{\nu_t} + \tilde{\nu}_t)\left[\frac{\partial(U_i + \tilde{u}_i)}{\partial x_j} + \frac{\partial(U_j + \tilde{u}_j)}{\partial x_i}\right] \quad (2)$$

After Eq. (2) is introduced into Eqs. (1), several assumptions are made on the scales of the different variables to simplify the equations. In particular, the longitudinal velocity U is normalized with U_0 (peak speed in the duct), ρU_0^2 is used as scale for $P^* = P + P_T$, duct length L is used as streamwise scale ($L \gg h$), and h is cross-stream scale. Thus, the leading-order terms of the streamwise momentum equation (1) give rise to

$$0 = -\frac{1}{\rho}\frac{\mathrm{d}P^*}{\mathrm{d}x} + \nu(U_{yy} + U_{zz}) + (\bar{\nu}_t U_y)_y + (\bar{\nu}_t U_z)_z \quad (3)$$

together with no-slip boundary conditions for U at the walls. Further scales to be employed for the terms left at higher orders are h/ϵ for x (with ϵ a small parameter to be chosen), h for y and z, $\tilde{U}$ for $\tilde{u}$ ($\tilde{U}$ an unspecified velocity scale for the coherent terms, which is much smaller than U_0 and u_τ, the latter being the friction velocity, an appropriate scale for the fluctuations), $\epsilon\tilde{U}$ for $\tilde{v}$ and $\tilde{w}$, $\epsilon^2\rho\tilde{U}U_0$ for $\tilde{p}$. Furthermore, a classical analogy with kinetic theory suggests that $\bar{\nu}_t$ is of order hu_τ, so that $\tilde{\nu}_t$ scales with $hu_\tau\tilde{U}/U_0$.

By so doing, the different orders of magnitudes of the terms left in system (1) [after subtracting Eq. (3)] are

$$\underbrace{\tilde{u}_x+\tilde{v}_y+\tilde{w}_z=0}_{\mathcal{O}(\epsilon\tilde{U}/h)}$$

$$\underbrace{U\tilde{u}_x+\tilde{v}U_y+\tilde{w}U_z}_{\mathcal{O}(\epsilon\tilde{U}U_0/h)}=\underbrace{-\tilde{p}_x/\rho}_{\mathcal{O}(\epsilon^3\tilde{U}U_0/h)}+\underbrace{\nu\tilde{u}_{xx}}_{\mathcal{O}(\epsilon^2\nu\tilde{U}/h^2)}+\underbrace{\nu(\tilde{u}_{yy}+\tilde{u}_{zz})}_{\mathcal{O}(\nu\tilde{U}/h^2)}$$
$$+\underbrace{(\bar{\nu}\tilde{u}_x)_x}_{\mathcal{O}(\epsilon^2\tilde{U}u_\tau/h)}+\underbrace{(\bar{\nu}_t\tilde{u}_y+\tilde{\nu}_tU_y)_y+(\bar{\nu}_t\tilde{u}_z+\tilde{\nu}_tU_z)_z}_{\mathcal{O}(\tilde{U}u_\tau/h)}$$

$$\underbrace{U\tilde{v}_x}_{\mathcal{O}(\epsilon^2\tilde{U}U_0/h)}=\underbrace{-\tilde{p}_y/\rho}_{\mathcal{O}(\epsilon^2\tilde{U}U_0/h)}+\underbrace{\nu\tilde{v}_{xx}}_{\mathcal{O}(\epsilon^3\nu\tilde{U}/h^2)}+\underbrace{\nu(\tilde{v}_{yy}+\tilde{v}_{zz})}_{\mathcal{O}(\epsilon\nu\tilde{U}/h^2)}$$
$$+\underbrace{(\bar{\nu}_t\tilde{u}_y+\tilde{\nu}_tU_y)_x+(2\bar{\nu}_t\tilde{v}_y)_y+[\bar{\nu}_t(\tilde{v}_z+\tilde{w}_y)]_z}_{\mathcal{O}(\epsilon\tilde{U}u_\tau/h)}$$

$$\underbrace{U\tilde{w}_x}_{\mathcal{O}(\epsilon^2\tilde{U}U_0/h)}=\underbrace{-\tilde{p}_z/\rho}_{\mathcal{O}(\epsilon^2\tilde{U}U_0/h)}+\underbrace{\nu\tilde{w}_{xx}}_{\mathcal{O}(\epsilon^3\nu\tilde{U}/h^2)}+\underbrace{\nu(\tilde{w}_{yy}+\tilde{w}_{zz})}_{\mathcal{O}(\epsilon\nu\tilde{U}/h^2)}$$
$$+\underbrace{(\bar{\nu}_t\tilde{u}_z+\tilde{\nu}_tU_z)_x+[\bar{\nu}_t(\tilde{v}_z+\tilde{w}_y)]_y+(2\bar{\nu}_t\tilde{w}_z)_z}_{\mathcal{O}(\epsilon\tilde{U}u_\tau/h)} \tag{4}$$

The small parameter ϵ results by imposing the requirement that the Reynolds stress terms are of the same order of the convective terms,[23] so that the ratio between the cross stream and the streamwise length scale is

$$\epsilon=u_\tau/U_0$$

This results agrees with that of Mellor[23] for the external region of a turbulent boundary layer (the so-called *defect layer*). In the near-wall region a different ratio of length scales can be found by comparing the Reynolds-stress term to the viscous term; however, in the present case, rather than building separate approximations in the wall layer and in the defect layer, we use a composite approximation by retaining the leading viscous terms (even if formally negligible since $\epsilon\gg\nu/U_0h=Re^{-1}$ except very close to the walls) in the equations above. Finally, the following dimensional system of equations for the coherent flow is obtained:

$$\tilde{u}_x+\tilde{v}_y+\tilde{w}_z=0$$

$$U\tilde{u}_x+\tilde{v}U_y+\tilde{w}U_z=\nu(\tilde{u}_{yy}+\tilde{u}_{zz})+(\bar{\nu}_t\tilde{u}_y+\tilde{\nu}_tU_y)_y$$
$$+(\bar{\nu}_t\tilde{u}_z+\tilde{\nu}_tU_z)_z$$

$$U\tilde{v}_x=-\tilde{p}_y/\rho+\nu(\tilde{v}_{yy}+\tilde{v}_{zz})+(\bar{\nu}_t\tilde{u}_y+\tilde{\nu}_tU_y)_x$$
$$+(2\bar{\nu}_t\tilde{v}_y)_y+[\bar{\nu}_t(\tilde{v}_z+\tilde{w}_y)]_z$$

$$U\tilde{w}_x=-\tilde{p}_z/\rho+\nu(\tilde{w}_{yy}+\tilde{w}_{zz})+(\bar{\nu}_t\tilde{u}_z+\tilde{\nu}_tU_z)_x$$
$$+[\bar{\nu}_t(\tilde{v}_z+\tilde{w}_y)]_y+(2\bar{\nu}_t\tilde{w}_z)_z \tag{5}$$

To close them a suitable representation for turbulent viscosity must be found. The original hypothesis by Boussinesq[24] was that ν_t was approximately constant, and indeed reasonably good agreement with simple shear flows (jets and wakes) can be found by employing a constant eddy viscosity, whose value is 10–100 times the laminar value. A Newtonian eddy viscosity was also used by Reynolds and Hussain.[19] In the presence of boundaries, a kinetic-theory-like assumption gives

$$\nu_t=c_1\,\mathrm{rms}(u)l_m$$

with c_1 an order-one constant, $\mathrm{rms}(u)$ a measure of the rms velocity, such as the friction velocity u_τ, and l_m a dispersion length scale called *mixing length*. Bearing in mind the inherent limitations of mixing length models,[25] we limit ourselves here to the simplest possible closure by writing

$$\nu_t=\bar{\nu}_t+\tilde{\nu}_t=c_2(U+\tilde{u})l_m$$

with c_2 a constant (function of the Reynolds number of the flow) and l_m a function of position, defined as the harmonic mean of the distance of any given point in a quadrant from the two orthogonal walls. In particular, if η (respectively ψ) represents the distance of a given point from the nearest wall parallel to the y axis (z axis), we impose

$$l_m=2[\eta\psi/(\eta+\psi)]$$

Through this definition the mixing length is very small whenever a point is in proximity of a wall, and becomes close to the arithmetic mean of η and ψ when the two lengths become of comparable size.

Because it is not the point of the present paper to focus on turbulence closure models, we satisfy ourselves with the simple approximation above; we refer to Mompean[26] for recent developments on linear and nonlinear closure strategies aimed at capturing corner vortices.

For convenience, Eqs. (3) and (5) are rendered dimensionless. This is done by employing h as a length scale, U_0 as a scale for all velocity components, and ρU_0^2 as a scale for both P^* and $\tilde{p}$. Without changing notations between dimensional and dimensionless variables, the equations now read

$$0=-\frac{\mathrm{d}P^*}{\mathrm{d}x}+\frac{1}{Re}(U_{yy}+U_{zz})+(\hat{\bar{\nu}}_tU_y)_y+(\hat{\bar{\nu}}_tU_z)_z \tag{6}$$

$$\tilde{u}_x+\tilde{v}_y+\tilde{w}_z=0$$

$$U\tilde{u}_x+\tilde{v}U_y+\tilde{w}U_z=\frac{1}{Re}(\tilde{u}_{yy}+\tilde{u}_{zz})+(\hat{\tilde{\nu}}_t\tilde{u}_y+\hat{\tilde{\nu}}_tU_y)_y$$
$$+(\hat{\tilde{\nu}}_t\tilde{u}_z+\hat{\tilde{\nu}}_tU_z)_z$$

$$U\tilde{v}_x=-\tilde{p}_y+\frac{1}{Re}(\tilde{v}_{yy}+\tilde{v}_{zz})+(\hat{\tilde{\nu}}_t\tilde{u}_y+\hat{\tilde{\nu}}_tU_y)_x+(2\hat{\tilde{\nu}}_t\tilde{v}_y)_y$$
$$+[\hat{\tilde{\nu}}_t(\tilde{v}_z+\tilde{w}_y)]_z$$

$$U\tilde{w}_x=-\tilde{p}_z+\frac{1}{Re}(\tilde{w}_{yy}+\tilde{w}_{zz})+(\hat{\tilde{\nu}}_t\tilde{u}_z+\hat{\tilde{\nu}}_tU_z)_x$$
$$+[\hat{\tilde{\nu}}_t(\tilde{v}_z+\tilde{w}_y)]_y+(2\hat{\tilde{\nu}}_t\tilde{w}_z)_z \tag{7}$$

with $\hat{\nu}_t=\nu_t/\nu=\hat{\bar{\nu}}_t+\hat{\tilde{\nu}}_t$.

III. Unidirectional Motion U

To solve for U we simply impose the pressure gradient $\mathrm{d}P^*/\mathrm{d}x$, for example, on the value calculated by Gavrilakis[6] at $Re=2933$ (hence $\mathrm{d}P^*/\mathrm{d}x=-15.3463$), and discretize Eq. (6). The unknown are the values of $U(y,z)$ at the $N\times N$ Gauss–Lobatto grid points, $y_i=\cos\pi(i-1)/(N-1)$ with $i=1,\ldots,N$ and $z_j=\cos\pi(j-1)/(N-1)$ with $j=1,\ldots,N$. For instance, if U_{ij} denotes U at the grid point (y_i,z_j) the approximation adopted is

$$U(y,z)=\sum_{i=1}^{N}\sum_{j=1}^{N}U_{ij}\phi_i(y)\phi_j(z)$$

where $\phi_i(y)$ and $\phi_j(z)$ are the Lagrangian interpolating polynomials based on the nodes y_i and z_j, respectively. The internal nodal values

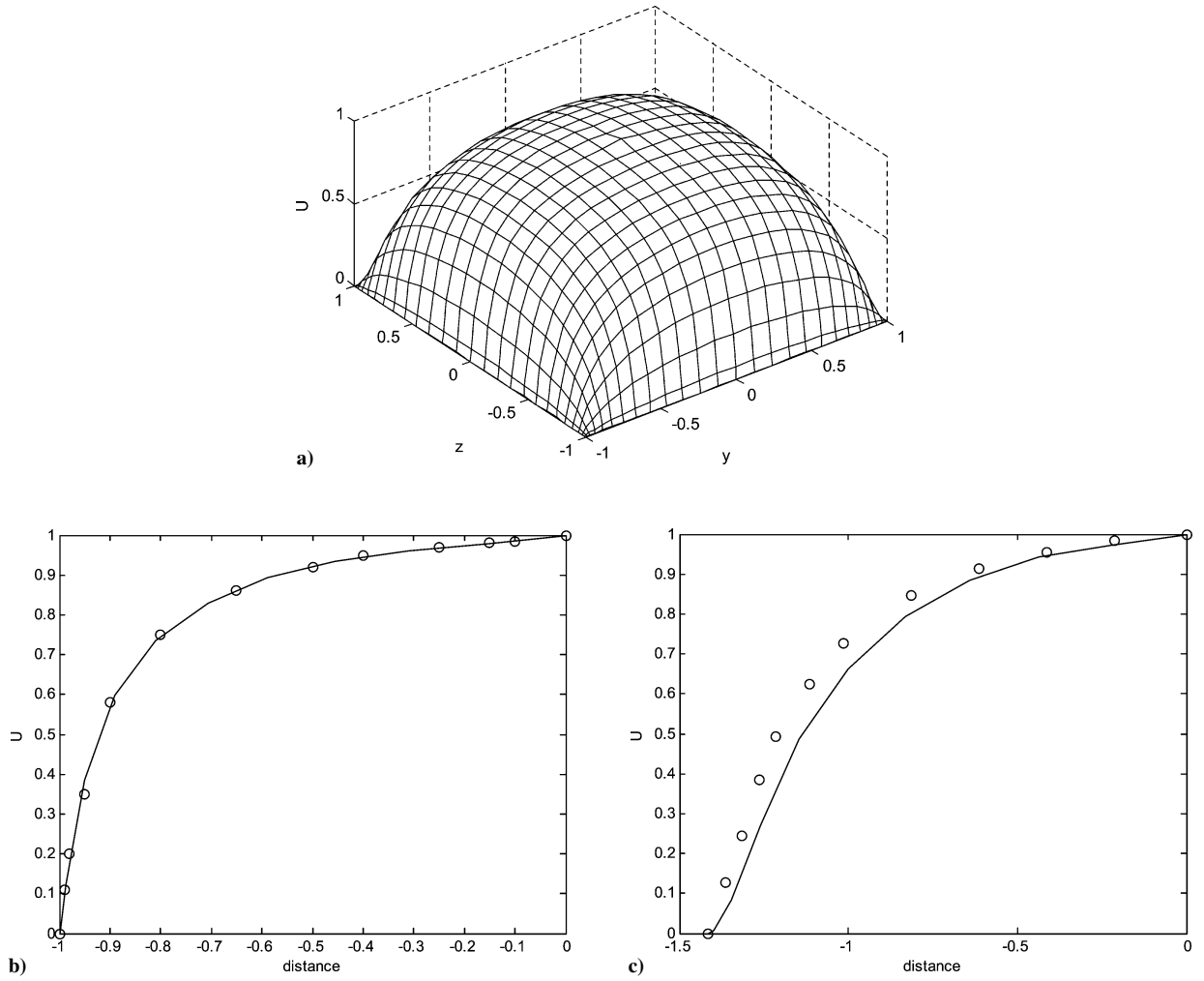

Fig. 2 Solution of Eq. (6) for the mean flow: a) surface plot of $U(y,z)$ in the duct cross section. Comparisons with the mean speed profile computed by Gavrilakis[6] (circles) along a bisection line y or $z=0$ (panel b) and along a diagonal (panel c) display acceptable agreement. Observe that the result by Gavrilakis also includes $\tilde{u}$.

of U are arranged into a vector $\boldsymbol{U}$, and the discrete form of Eq. (6) is solved with a simple iterative technique.

Numerical tests show that fitting the constant c_2 to the value of 22 (which indicates by how much the turbulent viscosity exceeds the kinematic viscosity near the centerline of the duct) produces acceptable results for U, displayed in Fig. 2.

IV. Functional Optimization for Coherent Motion

A. Cost Functionals and Energy Constraint

The choice of which cost functional we should maximize is crucial because it affects the results obtained and their interpretation. In stability theory it is customary to consider the disturbance kinetic energy density as a suitable cost (see, for example, Tumin and Ashpis[27]); also in the present case, the first thing attempted by Galletti and Bottaro[16] was the optimization at a given downstream position L of an energylike norm $\mathcal{I}(L)$ related to the streaky motion, with

$$\mathcal{I}(x) = \frac{1}{2}\int_{-1}^{1}\int_{-1}^{1} \tilde{u}(x,y,z)^2 \,\mathrm{d}y\,\mathrm{d}z \tag{8}$$

for a given initial energy. On second thought, there are other functionals that might perhaps better represent the behavior of turbulent flows in ducts. It has been suggested by Malkus[17] and later elaborated by Busse[28] that turbulence achieves statistical extreme states related to the degree of disorganization, or entropy, of the process. In statistically steady shear flow, the temperature of the fluid relative to the walls can reach a maximum value when the rate of viscous dissipation of energy into heat is largest. This seems to imply that a sensible quantity to optimize is the cross-sectional integral of the turbulent dissipation function ϕ_v, that is,

$$\int_{-1}^{1}\int_{-1}^{1} \phi_v \,\mathrm{d}y\,\mathrm{d}z = \frac{1}{Re}\int_{-1}^{1}\int_{-1}^{1} 2\overline{s'_{ij}s'_{ij}}\,\mathrm{d}y\,\mathrm{d}z$$

with

$$s'_{ij} = \frac{1}{2}\left(\frac{\partial u'_i}{\partial x_j} + \frac{\partial u'_j}{\partial x_i}\right)$$

the fluctuating rate of strain. This quantity is indispensable to the dynamics of turbulence and recent results by Plasting and Kerswell[29] have shown that the solutions maximizing the dissipation rate bear some resemblance to turbulent flows realized in a pipe.[12] Usually, the fluctuating strain rate is much larger than the mean strain rate

$$s'_{ij} \gg S_{ij} = \frac{1}{2}\left[\frac{\partial(U_i+\tilde{u}_i)}{\partial x_j} + \frac{\partial(U_j+\tilde{u}_j)}{\partial x_i}\right]$$

indicating that the eddies contributing the most to the dissipation of energy have very small convective time scales compared to those of the mean flow. In the present context, adopting an objective function based on $\overline{s'_{ij}s'_{ij}}$ entails relying heavily on the adopted model for the

Reynolds stress and produces a very complicated expression. However, if we assume that, on average, the rate of energy dissipation and the work of deformation of the mean motion by the Reynolds stresses are equal, that is, that there is mechanical-energy equilibrium, the viscous dissipation can be estimated from the large-scale dynamics. Thus, an equally important cost functional to consider is the turbulent energy production per unit mass:

$$\mathcal{P}(x) = -\int_{-1}^{1}\int_{-1}^{1} \overline{u_i' u_j'} S_{ij}\,\mathrm{d}y\,\mathrm{d}z$$

By introducing the Boussinesq assumption (2), the rate of production at leading order is given by

$$\int_{-1}^{1}\int_{-1}^{1} \hat{\tilde{\nu}}_t \frac{\partial U_i}{\partial x_j}\frac{\partial U_j}{\partial x_i} + \hat{\tilde{\nu}}_t \left(\frac{\partial U_j}{\partial x_i}\right)^2 + \hat{\tilde{\nu}}_t \frac{\partial U_j}{\partial x_i}\frac{\partial \tilde{u}_i}{\partial x_j} + \hat{\tilde{\nu}}_t \frac{\partial U_j}{\partial x_i}\frac{\partial \tilde{u}_j}{\partial x_i}\,\mathrm{d}y\,\mathrm{d}z$$

Assuming that the eddy viscosity $\hat{\nu}_t$ is given, a suitable cost is then

$$\int_{-1}^{1}\int_{-1}^{1} \frac{\partial U_j}{\partial x_i}\frac{\partial \tilde{u}_i}{\partial x_j} + \frac{\partial U_j}{\partial x_i}\frac{\partial \tilde{u}_j}{\partial x_i}\,\mathrm{d}y\,\mathrm{d}z$$

which reduces in the present case to

$$\int_{-1}^{1}\int_{-1}^{1} (U_y \tilde{u}_y + U_z \tilde{u}_z)\,\mathrm{d}y\,\mathrm{d}z$$

However, it is easy to see that this integral goes to zero because of the symmetry properties of the coherent motion around diagonals and/or bisection lines, so that an appropriate functional to maximize must be sought at next higher order, and reads

$$\mathcal{I}(x) = \int_{-1}^{1}\int_{-1}^{1} \left(\tilde{u}_y^2 + \tilde{u}_z^2\right)\mathrm{d}y\,\mathrm{d}z \tag{9}$$

The weak point of this argument lies in the statement that $\hat{\nu}_t$ is assumed as a datum; we could equally well have assumed a functional dependence of $\hat{\nu}_t$ on the mean flow $U_i + \tilde{u}_i$ (as we did in the preceding section when closing the direct problem to search for a numerical solution), thus obtaining a different cost function. In the search of a suitable objective, however, we prefer not to use a model of the eddy viscosity and consider it as a property of small scale, incoherent processes. This assumption has the advantage of producing a functional that is not unnecessarily complicated. Different types of functionals have also been optimized, extensively discussed by Soueid,[30] producing results qualitatively similar to those discussed in the following.

When an energylike norm is chosen, such as

$$E(x) = \frac{1}{2}\int_{-1}^{1}\int_{-1}^{1} \tilde{u}(x,y,z)^2 + \epsilon^2[\tilde{v}(x,y,z)^2 + \tilde{w}(x,y,z)^2]\,\mathrm{d}y\,\mathrm{d}z$$

(the term ϵ^2 is present because of the different scales of the velocity components), it is easy to see[31] that an inflow with $\tilde{u}(0,y,z) = 0$ yields a gain (ratio of outlet to inlet norm) which is asymptotically large and of order ϵ^{-2}. In this case, combining the first two equations of set (7) to eliminate $\tilde{u}_x$, one finds that at $x = 0$ the variables $\tilde{v}$ and $\tilde{w}$ are related by

$$U\tilde{v}_y + U\tilde{w}_z = \tilde{v}U_y + \tilde{w}U_z$$

so that there are only two independent initial conditions to apply, $\tilde{u}$, which vanishes, and $\tilde{v}$, which comes out of the optimization procedure. The other velocity component at the inlet, $\tilde{w}$, must be assigned by the use of the preceding equation.

For all functionals studied we have thus decided to constrain the initial energy norm as follows:

$$E_0 = \frac{1}{2}\int_{-1}^{1}\int_{-1}^{1} [\tilde{v}(0,y,z)^2 + \tilde{w}(0,y,z)^2]\,\mathrm{d}y\,\mathrm{d}z = 1$$

with $\tilde{u}(0,y,z) = 0$.

B. Discrete Problem for the Coherent State

The unknowns contained in Eq. (7) are treated in a manner similar to the variable U, that is, by introducing Gauss–Lobatto grid points and Lagrangian interpolating polynomials. By denoting as $\boldsymbol{p}$, $\boldsymbol{u}$, $\boldsymbol{v}$, and $\boldsymbol{w}$ the column vectors containing the interior nodal values of $\tilde{p}$, $\tilde{u}$, $\tilde{v}$, and $\tilde{w}$, the discretized form of Eqs. (7) can be written as

$$\boldsymbol{Q}\boldsymbol{q}_x = \boldsymbol{R}\boldsymbol{q} \tag{10}$$

where $\boldsymbol{q} = [\boldsymbol{p}, \boldsymbol{u}, \boldsymbol{v}, \boldsymbol{w}]^T$ is a $4M \times 1$ vector and $\boldsymbol{Q}$ and $\boldsymbol{R}$ are $4M \times 4M$ matrices of the form

$$\boldsymbol{Q} = \begin{pmatrix} 0 & 0 & 0 & 0 \\ 0 & Q_{22} & 0 & 0 \\ 0 & Q_{32} & Q_{33} & 0 \\ 0 & Q_{42} & 0 & Q_{44} \end{pmatrix}, \qquad \boldsymbol{R} = \begin{pmatrix} 0 & R_{12} & R_{13} & R_{14} \\ 0 & R_{22} & R_{23} & R_{24} \\ R_{31} & 0 & R_{33} & R_{34} \\ R_{41} & 0 & R_{43} & R_{44} \end{pmatrix}$$

obtained after multiplying the continuity equation by U and then subtracting the result from the x-momentum equation (see Soueid[30] for details). All of the $M \times M$ submatrices R_{ij} are singular for $i \neq j$. $M = (N-2)\times(N-2)$ is the total number of interior nodes and the no-slip boundary conditions are enforced implicitly. The initial conditions arise from the optimization, however, for the cases of $\boldsymbol{p}$ and $\boldsymbol{u}$ we simply impose vanishing values. (This is justified for the case of $\boldsymbol{p}$ by the fact that there is no streamwise pressure coupling for the variable $\tilde{p}$.) Along the streamwise direction an implicit finite difference discretization is adopted, of second order except for the first step, so that the discrete problem reads

$$\boldsymbol{q}_0 = [\boldsymbol{0}, \boldsymbol{0}, \boldsymbol{v}(0), \boldsymbol{w}(0)]^T, \qquad \boldsymbol{q}_1 = \boldsymbol{G}_1\boldsymbol{q}_0$$

$$\boldsymbol{q}_{n+1} = \boldsymbol{G}_2(4\boldsymbol{q}_n - \boldsymbol{q}_{n-1}), \qquad n = 1, \ldots, N_L - 1 \tag{11}$$

where $\boldsymbol{q}_n = \boldsymbol{q}(n\Delta x)$, $\boldsymbol{G}_1 = (\boldsymbol{Q} - \boldsymbol{R}\Delta x)^{-1}\boldsymbol{Q}$, $\boldsymbol{G}_2 = (3\boldsymbol{Q} - 2\boldsymbol{R}\Delta x)^{-1}\boldsymbol{Q}$, and $L = N_L\Delta x$ is the length of the channel. The expressions $\boldsymbol{Q} - \boldsymbol{R}\Delta x$ and $3\boldsymbol{Q} - 2\boldsymbol{R}\Delta x$ are singular matrices, and to obtain $\boldsymbol{G}_1$ and $\boldsymbol{G}_2$ we must resort to an inversion procedure based on singular value decomposition. Any square matrix can be expressed as the product of an orthogonal matrix $\boldsymbol{U}$, a diagonal matrix $\boldsymbol{W}$ with the singular values w_i on the diagonal elements arranged in decreasing order, and the transpose of a second orthogonal matrix $\boldsymbol{V}$. The inverse of the matrix is then simply the product

$$\boldsymbol{V}[\mathrm{diag}(1/w_i)]\boldsymbol{U}^T$$

and if a singular value w_i vanishes or nearly vanishes (a signal of matrix singularity or poor conditioning) we simply replace $1/w_i$ with zero in this expression.[32] This procedure has been adopted successfully in the present case and validated by comparing it to an alternative procedure based on the reduction of the order the matrices.[16] Numerical tests reveal that $\Delta x = 2.2$ produces converged results, together with $N = 23$ collocation points along y and z. This is demonstrated in Fig. 3, where the quantity

$$E_T = \frac{1}{2L}\int_{-1}^{1}\int_{-1}^{1}\int_{0}^{L} \tilde{u}(x,y,z)^2\,\mathrm{d}x\,\mathrm{d}y\,\mathrm{d}z$$

arising from several direct calculations at different resolutions is reported for an initial condition at $x = 0$ given by

$$\tilde{u}(0,y,z) = 0, \qquad \tilde{v}(0,y,z) = U(y,z)[\cos\pi z + \cos\pi(y-z)]$$

The cost function is written in a generic way:

$$\mathcal{J} = \alpha_1\mathcal{I}(L) + \frac{\alpha_2}{L}\int_0^L \mathcal{I}(x)\,\mathrm{d}x$$

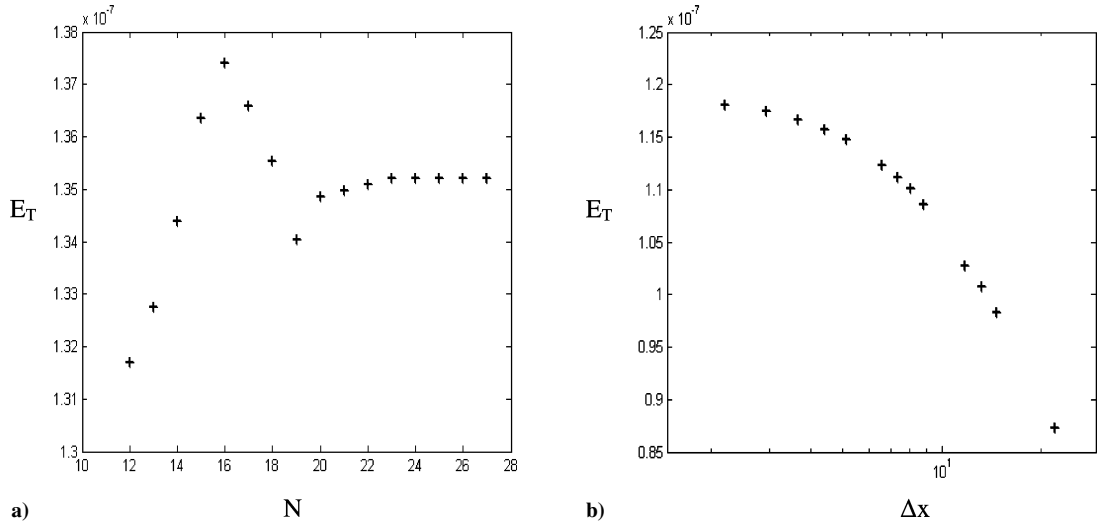

Fig. 3 Grid resolution study: a) streamwise step fixed at $\Delta x = 2.2$ with $L = 220$ and b) all calculations performed with $N = 23$ and $L = 396$.

to either target $\mathcal{I}$ at the final position (when $\alpha_2 = 0$) or as an integral over x (when $\alpha_1 = 0$). The former option has been used in most of the studies on optimal perturbations to date.[33] In discrete form, this cost has the form

$$\mathcal{J}_n = \frac{1}{2}\alpha_1 \boldsymbol{q}_{N_L}^T \boldsymbol{A}\boldsymbol{q}_{N_L} + \frac{\alpha_2}{2L}\sum_{n=1}^{N_L} \boldsymbol{q}_n^T \boldsymbol{A}\boldsymbol{q}_n \Delta x \tag{12}$$

with the $4M \times 4M$ matrix $\boldsymbol{A}$ containing both a filter, to account for the choice of $\mathcal{J}$ [either Eq. (8) or Eq. (9)], and quadrature weights.[34]

In the discrete setting the constraint on the initial energy norm can be expressed as

$$\tfrac{1}{2}\boldsymbol{q}_0^T \boldsymbol{B}\boldsymbol{q}_0 = E_0 \tag{13}$$

with the $4M \times 4M$ matrix $\boldsymbol{B}$ containing, as before, a filter to go from the vector $\boldsymbol{q}$ to the vectors $\boldsymbol{v}$ and $\boldsymbol{w}$ needed to compute E_0, and quadrature weights.

Applying a methodology based on Lagrange multipliers,[35] the constrained optimization problem is transformed into an unconstrained one for the extended, discrete functional:

$$\begin{aligned}\mathcal{L}_n = {} & \frac{1}{2}\alpha_1 \boldsymbol{q}_{N_L}^T \boldsymbol{A}\boldsymbol{q}_{N_L} + \boldsymbol{r}_0^T(\boldsymbol{q}_1 - \boldsymbol{G}_1\boldsymbol{q}_0) \\ & + \sum_{n=1}^{N_L-1}\left\{\boldsymbol{r}_n^T[\boldsymbol{q}_{n+1} - \boldsymbol{G}_2(4\boldsymbol{q}_n - \boldsymbol{q}_{n-1})] + \frac{\alpha_2}{2L}\boldsymbol{q}_n^T\boldsymbol{A}\boldsymbol{q}_n\Delta x\right\} \\ & + \frac{\alpha_2}{2L}\boldsymbol{q}_{N_L}^T\boldsymbol{A}\boldsymbol{q}_{N_L}\Delta x + \lambda_0\left(\frac{1}{2}\boldsymbol{q}_0^T\boldsymbol{B}\boldsymbol{q}_0 - E_0\right)\end{aligned}$$

with $\boldsymbol{r}$ a $4M \times 1$ vector of Lagrange multipliers and λ_0 a scalar multiplier needed to force the initial energy norm to the given value $E_0 = 1$. In a continuous setting, an adjoint set of equations is found by performing integration by parts[36]; in the present discrete setting it is sufficient to rewrite the functional in the equivalent form

$$\begin{aligned}\mathcal{L}_n = {} & \left[\frac{1}{2}\left(\alpha_1 + \frac{\alpha_2\Delta x}{L}\right)\boldsymbol{q}_{N_L}^T\boldsymbol{A} + \boldsymbol{r}_{N_L-1}^T\right]\boldsymbol{q}_{N_L} - \boldsymbol{r}_{N_L}^T\boldsymbol{G}_2\boldsymbol{q}_{N_L-1} \\ & - \lambda_0 E_0 + \left(\frac{\lambda_0}{2}\boldsymbol{q}_0^T\boldsymbol{B} - \boldsymbol{r}_0^T\boldsymbol{G}_1 + \boldsymbol{r}_1^T\boldsymbol{G}_2\right)\boldsymbol{q}_0 \\ & + \sum_{n=1}^{N_L-1}\left\{\boldsymbol{r}_{n-1}^T + \left[\boldsymbol{r}_{n+1}^T - 4\boldsymbol{r}_n^T\right]\boldsymbol{G}_2 + \frac{\alpha_2\Delta x}{2L}\boldsymbol{q}_n^T\boldsymbol{A}\right\}\boldsymbol{q}_n\end{aligned}$$

and enforce stationarity with respect to all independent variables to demonstrate that the direct system of discrete equations is coupled to a discrete adjoint system to be integrated backward in space. Such a system reads as follows:

$$\begin{aligned}&\boldsymbol{r}_{N_L} = [\boldsymbol{0}, \boldsymbol{0}, \boldsymbol{0}, \boldsymbol{0}]^T, \qquad \boldsymbol{r}_{N_L-1} = -[\alpha_1 + \Delta x(\alpha_2/L)]\boldsymbol{A}^T\boldsymbol{q}_{N_L} \\ &\boldsymbol{r}_{n-1} = \boldsymbol{G}_2^T(4\boldsymbol{r}_n - \boldsymbol{r}_{n+1}) - \Delta x(\alpha_2/L)\boldsymbol{A}^T\boldsymbol{q}_n, \qquad n = N_L - 1, \ldots, 1\end{aligned} \tag{14}$$

together with the optimality condition

$$\boldsymbol{q}_0 = \left(\lambda_0\boldsymbol{B}^T\right)^{-1}\left(\boldsymbol{G}_1^T\boldsymbol{r}_0 - \boldsymbol{G}_2^T\boldsymbol{r}_1\right)$$

This condition makes it possible to iteratively update the inflow solution of the direct problem on the basis of the adjoint solution at the streamwise nodes $n = 0$ and $n = 1$. The multiplier λ_0 is iteratively updated to enforce the constraint on E_0. Typically we perform up to 500 direct/adjoint iterations until the difference in $\mathcal{J}$ between two successive iterations is smaller than a given threshold. The need for such a large number of iterations arises from the fact that the functional often displays in the course of the iterations one or two plateaus before convergence, an indication of the weak selectivity of the optimal solution eventually achieved.

V. Results

A. Energy Functional

The variety of structures that appear upon optimizing the energylike norm of Eq. (8) at a final position ($\alpha_1 = 1, \alpha_2 = 0$) or as an integral over x ($\alpha_1 = 0, \alpha_2 = 1$) is displayed in Figs. 4 and 5. Although the norms achieved at any given L seem very small (cf. the values on the ordinate axis of the graphs) and further decreasing very steeply with the optimization distance L for the first case (for the latter a local maximum appears at $x = 15.5$, from which point on a mild monotonic decrease sets in toward what appears to be a limit value for L asymptotically large), they should still be multiplied by ϵ^{-2} to yield a number with physical relevance. As the distance from the inflow increases, structures with larger cross-stream dimensions are capable of optimally draining energy from U (Fig. 4). However, beyond a threshold value of L equal to about 300 half-channel thicknesses one and the same optimal solution is consistently found: eight vortices in the cross section, symmetric about the diagonals and the bisection lines, are capable of extracting the most energy out of U. In the case in which an integral measure is considered, eight vortices constitute the optimal disturbance over small distances, and progressively larger cross-stream structures make their appearance as L increases.

It can be speculated that, once a localized inhomogeneity has triggered a spatial transient in the duct, the flow evolves to select secondary patterns such as those displayed here, until nonlinear mixing

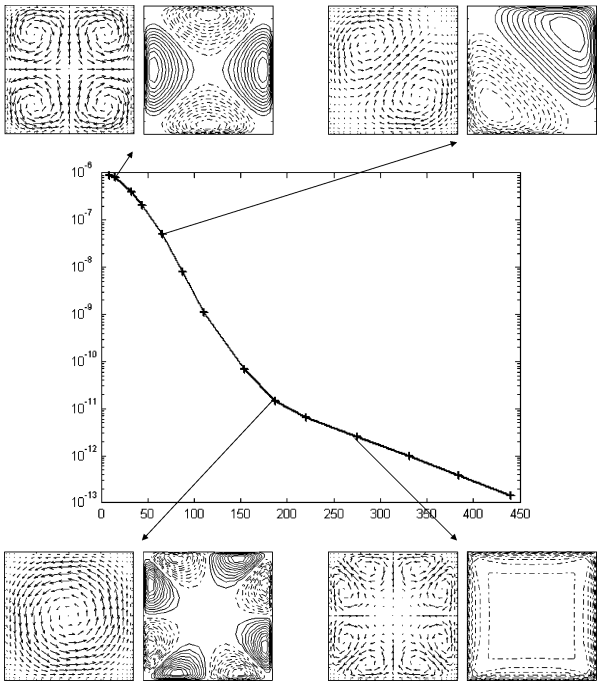

Fig. 4 Energy norm ($\alpha_1 = 1$, $\alpha_2 = 0$) as a function of the optimization distance, and corresponding solutions. The vector plots provide the optimal initial conditions $\tilde{v}$ and $\tilde{w}$ at $x = 0$, that is, that maximizing the energy at a prescribed length L; the contour plots are isolines of the streamwise velocity $\tilde{u}$ at the final position L. Dashed lines denote negative values of $\tilde{u}$.

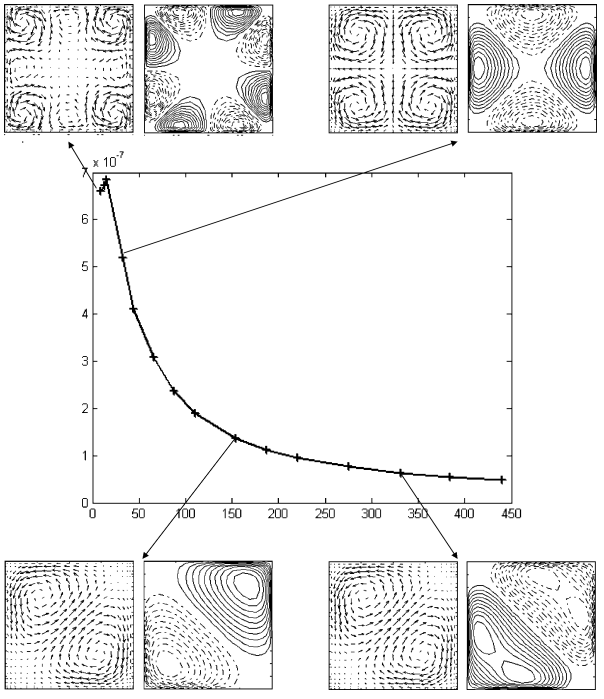

Fig. 5 Energy norm ($\alpha_1 = 0$, $\alpha_2 = 1$) as a function of the optimization distance, and corresponding solutions.

mechanisms become sufficiently vigorous to moderate, maintain, or regenerate coherence. We make no claims on how "optimal" cross-stream structures appear in a turbulent duct at some position (which in our reference frame is $x = 0$): this is a matter related to the flow receptivity and the response of the system to environmental forcing. We simply state that if vortices such as those found here are eventually present at some "initial" position in a square duct, a local or integral energy norm will be optimized downstream. It is thus appropriate at this point to look at a norm even loosely related to the dissipation rate, because this is the functional that Malkus[17] conjectured could be maximized during the development of a chaotic flow.

B. "Production" Functional

Results obtained by focusing on a "production" cost [Eq. (9)] are shown in Figs. 6 and 7. Figure 6, in particular, shows that the optimal organized motion is unique (and L dependent), irrespective of the

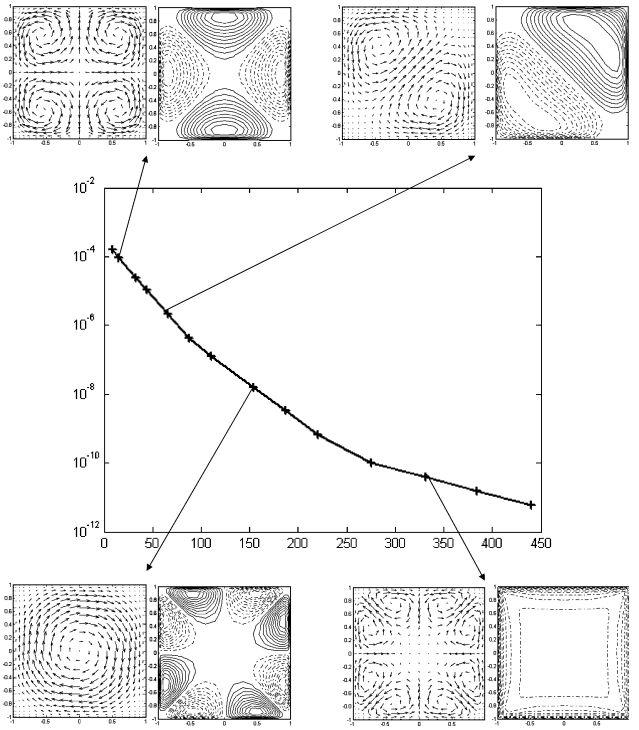

Fig. 6 Productionlike norm ($\alpha_1 = 1$, $\alpha_2 = 0$) as a function of the optimization distance, and corresponding solutions.

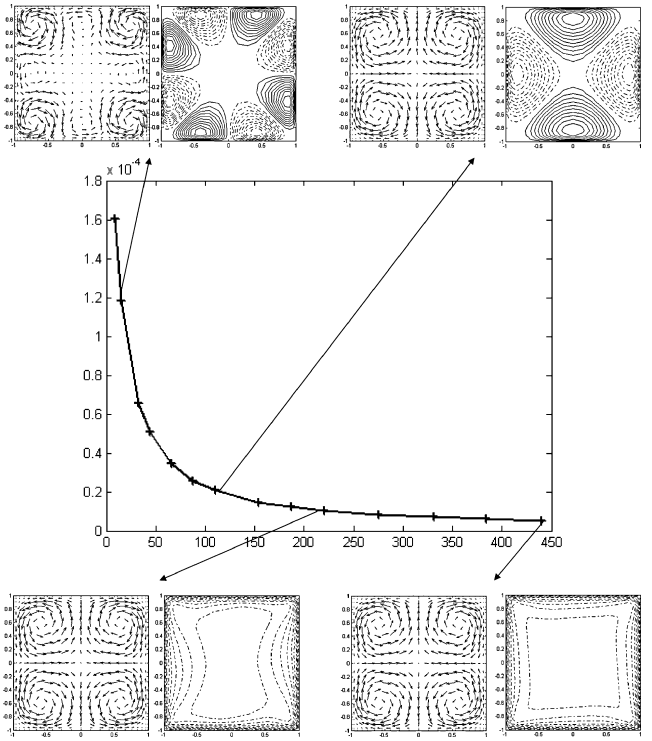

Fig. 7 Productionlike norm ($\alpha_1 = 0$, $\alpha_2 = 1$) as a function of the optimization distance, and corresponding solutions.

chosen cost, in optimizing a local quantity (cf. Fig. 4). This seems indicative of a "universal" behavior of the coherent field.

Also in the case of an integral measure the results are similar between the two objective functions (cf. Figs. 5 and 7), at least for small values of L. When L exceeds 100 there is a tendency of the "optimal" states for the integral measure to consistently exploit the symmetry around the bisection lines, rather than that around diagonals.

C. Discussion

A possible mechanism for the formation of secondary currents in a square duct has been presented.

The classical argument goes that streamwise vorticity can be produced in a streamwise homogeneous turbulent flow by the anisotropy of turbulence. In the context of the triple decomposition adopted here, the streamwise vorticity equation that follows from Eq. (1) reads

$$U\tilde{\omega}_x = \nu(\tilde{\omega}_{yy} + \tilde{\omega}_{zz}) + \underbrace{U_z\tilde{v}_x - U_y\tilde{w}_x}_{P_1} + \underbrace{(\overline{v'v'} - \overline{w'w'})_{yz}}_{P_2}$$

$$+ \underbrace{(\partial_{zz} - \partial_{yy})\overline{v'w'}}_{P_3} + \underbrace{\partial_x[(\overline{u'v'})_z - (\overline{u'w'})_y]}_{P_4} \tag{15}$$

so that, if the assumption of fully developed flow is made, the balance equation is

$$\tilde{v}\tilde{\omega}_y + \tilde{w}\tilde{\omega}_z = \nu(\tilde{\omega}_{yy} + \tilde{\omega}_{zz}) + P_2 + P_3 \tag{16}$$

where the (nonlinear) left-hand side has been included to account for the convection of the streamwise vorticity by the secondary flows. Experiments by Perkins[18] have demonstrated that the Reynolds stress terms P_2 and P_3 are in balance over the majority of the cross section, with the convective term significant near the corners and the viscous term very near the wall. A classical Boussinesq closure for P_2 and P_3 (with a constant eddy viscosity) would decouple Eq. (16) from the streamwise momentum equation, producing the solution $\tilde{v} = \tilde{w} = 0$, which is the reason that a nonlinear relation for the Reynolds stress tensor[8] has traditionally been considered indispensable.

The (conventional) assumption of streamwise invariance of the motion, however, removes two potential sources for the coherent field: in the context of the equation for ω such source terms are P_1, related to the mean shear skewing and present also in the laminar case, and P_4, which couples the equations for $\tilde{\omega}$ and $\tilde{u}$ even in the context of the simple Boussinesq assumption with constant ν_t. Thus, relaxing the homogeneity hypothesis implies not only that the secondary flows are maintained/enhanced by turbulence, but also that they can be produced during a spatial transient phase through interaction with the mean shear terms U_y and U_z. Transients dominate the dynamics of the flow whenever the system reacts to sudden inhomogeneities, such as roughness elements, that is, during receptivity phases. Furthermore, we argue that fully developed turbulence is just a (convenient) representation of a reality that is, in fact, a succession of transients. Clearly, the structures found would decay under the action of viscosity if it were not for a nonlinear mixing mechanism involving the coherent field (mechanism not considered here) that could maintain/regenerate/alter the secondary vortices, ultimately yielding the states observed in several simulations and experiments. Also, the anisotropy of turbulence near the walls (particularly through the action of the terms labeled P_2 and P_3) plays an important role in sustaining the secondary flows, and it is not the purpose of this work to play down the importance of such an effect.

On the negative side, we observe that the present conjecture on the initial stages of corner flows would be more appealing had we consistently found optimal states composed by eight vortices with symmetries about diagonals and bisection lines. Although it could be argued that we still need to account for the generic nonlinear mixer to describe fully developed states [in which case, however, the separation of scales between streamwise and cross-stream distances eventually leading to system (7) would be untenable] and that secondary flows with the right symmetries do not necessarily have to be expected during a transient, the results found leave us with mixed feelings. This must (at least in part) be ascribed to the choice of the functional and to the impossibility, within the present framework, of adequately representing the rate of turbulent energy dissipation ϕ_v or, for that matter, any measure related to incoherent fluctuations. Only a direct numerical simulation of turbulence capable of providing exactly the fluctuating rate of strain s'_{ij}, coupled to an optimization procedure, could provide a definite answer. Simulations of this kind have not yet been attempted.

VI. Conclusions

The optimization of coherent disturbances developing spatially in a duct bounded by four solid walls has been performed by a direct-adjoint technique based on linear equations. The procedure has been carried out with respect to two different functionals: a kinetic-energy-like norm of the coherent motion and a production-like norm of turbulent kinetic energy. The latter has been employed instead of the dissipation rate (which would have required too many assumptions to be truly significant) under the hypothesis that production and dissipation are in equilibrium. Because no significant differences have been found between the two costs tested, we are incapable at this stage of speaking in favor of the argument that turbulence is a process maximizing the rate of energy dissipation.

The approach was meant to elucidate aspects of the response of the system to spatial inhomogeneities and stems from the realization that large-scale steady coherent structures respond linearly to the mean shear. Even with the limitations imposed by the simple isotropic turbulence closure used here, we have been able to find optimal flow states with secondary currents, often reminiscent of those observed in full numerical simulations and experiments. Clearly, the present amplification mechanism is only of transient nature and nonlinear effects must eventually be accounted for to sustain the cross-stream flows, including in particular those effects arising from the anisotropy of turbulence near walls.

The relation between secondary flows and so-called "exact coherent states"[9–14] in square ducts remains to be established.

Acknowledgments

Several interesting discussions on the topic of this paper have taken place with M. Colombini and A. Stocchino. The work by HS was supported by a grant awarded by the University of Genoa.

References

[1]Nikuradse, J., "Untersuchungen über die Geschwindigkeitsverteilung in Turbulenten Strömungen," Ph.D. Dissertation, Univ. of Göttingen, Göttingen, Germany, 1926.

[2]Brundett, E., and Baines, W. D., "The Production and Diffusion of Vorticity in Duct Flow," *Journal of Fluid Mechanics*, Vol. 19, 1964, pp. 375–394.

[3]Gessner, F. B., "The Origin of Secondary Flow in Turbulent Flow Along a Corner," *Journal of Fluid Mechanics*, Vol. 58, 1973, pp. 1–25.

[4]Demuren, A. O., and Rodi, W., "Calculation of Turbulence-Driven Secondary Motion in Non-Circular Ducts," *Journal of Fluid Mechanics*, Vol. 140, 1984, pp. 189–222.

[5]Madabhushi, R. K., and Vanka, S. P., "Large Eddy Simulation of Turbulence-Driven Secondary Flow in a Square Duct," *Physics of Fluids A*, Vol. 3, No. 11, 1991, pp. 2734–2745.

[6]Gavrilakis, S., "Numerical Simulation of Low Reynolds-Number Turbulent Flow Through a Straight Square Duct," *Journal of Fluid Mechanics*, Vol. 244, 1992, pp. 101–129.

[7]Townsend, A. A., *The Structure of Turbulent Shear Flow*, Cambridge Univ. Press, Cambridge, England, U.K., 1956.

[8]Speziale, C. G., "On Nonlinear k–l and k–ϵ Models of Turbulence," *Journal of Fluid Mechanics*, Vol. 178, 1987, pp. 459–475.

[9]Nagata, M., "Three-Dimensional Finite-Amplitude Solutions in Plane Couette Flow: Bifurcation from Infinity," *Journal of Fluid Mechanics*, Vol. 217, 1990, pp. 519–527.

[10]Waleffe, F., "Exact Coherent Structures in Channel Flow," *Journal of Fluid Mechanics*, Vol. 435, 2001, pp. 93–102.

[11]Waleffe, F., "Homotopy of Exact Coherent Structures in Plane Shear Flows," *Physics of Fluids*, Vol. 15, No. 6, 2003, pp. 1517–1534.

[12]Hof, B., van Doorne, C. W. H., Westerweel, J., Nieuwstadt, F. T. M., Faisst, H., Eckhardt, B., Wedin, H., Kerswell, R. R., and Waleffe, F., "Experimental Observation of Nonlinear Traveling Waves in Turbulent Pipe Flow," *Science*, Vol. 305, No. 5690, 2004, pp. 1594–1598.

[13]Faisst, H., and Eckhardt, B., "Travelling Waves in Pipe Flow," *Physical Review Letters*, Vol. 91, No. 22, 2003, p. 224502.

[14]Wedin, H., and Kerswell, R. R., "Exact Coherent Structures in Pipe Flow: Travelling Wave Solutions," *Journal of Fluid Mechanics*, Vol. 508, 2004, pp. 333–371.

[15]Kawahara, G., and Kida, S., "Periodic Motion Embedded in Plane Couette Turbulence: Regeneration Cycle and Burst," *Journal of Fluid Mechanics*, Vol. 449, 2001, pp. 291–300.

[16]Galletti, B., and Bottaro, A., "Large-Scale Secondary Structures in Duct Flow," *Journal of Fluid Mechanics*, Vol. 512, 2004, pp. 85–94.

[17]Malkus, W. V. R., "Outline of a Theory of Turbulent Shear Flow," *Journal of Fluid Mechanics*, Vol. 1, 1956, pp. 521–539.

[18]Perkins, H. J., "The Formation of Streamwise Vorticity in Turbulent Flow," *Journal of Fluid Mechanics*, Vol. 44, 1970, pp. 721–740.

[19]Reynolds, W. C., and Hussain, A. K. M. F., "The Mechanics of an Organized Wave in Turbulent Shear Flow. 3. Theoretical Models and Comparisons with Experiments," *Journal of Fluid Mechanics*, Vol. 54, 1972, pp. 263–288.

[20]Reau, N., and Tumin, A., "On Harmonic Perturbations in a Turbulent Mixing Layer," *European Journal of Mechanics B, Fluids*, Vol. 21, No. 2, 2002, pp. 143–155.

[21]Reau, N., and Tumin, A., "Harmonic Perturbations in Turbulent Wakes," *AIAA Journal*, Vol. 40, No. 3, 2002, pp. 526–530.

[22]Lifshitz, Y., Degani, D., and Tumin, A., "On Harmonic Perturbations in a Turbulent Mixing Layer," AIAA Paper 2004-2653, 2004.

[23]Mellor, G. L., "The Large Reynolds Number, Asymptotic Theory of Turbulent Boundary Layers," *International Journal of Engineering Science*, Vol. 10, No. 10, 1972, pp. 851–873.

[24]Boussinesq, J., "Essai sur la theorie des eaux courantes," *Mémoires Présentés par Divers Savants à l'Académie des Sciences, Paris*, Vol. 23, No. 1, 1877, pp. 1–660.

[25]Tennekes, H., and Lumley, J., *A First Course in Turbulence*, MIT Press, Cambridge, MA, 1972.

[26]Mompean, G., "Numerical Simulation of a Turbulent Flow near a Right-Angled Corner Using the Speziale Non-Linear Model with RNG k–ϵ Equations," *Computer and Fluids*, Vol. 27, No. 7, 1998, pp. 847–859.

[27]Tumin, A., and Ashpis, D. E., "Optimal Disturbances in Boundary Layers Subject to Streamwise Pressure Gradient," *AIAA Journal*, Vol. 41, No. 11, 2003, pp. 2297–2300.

[28]Busse, F. H., "Bounds for Turbulent Shear Flow," *Journal of Fluid Mechanics*, Vol. 41, 1970, pp. 219–240.

[29]Plasting, S. C., and Kerswell, R. R., "A Friction Factor Bound for Transitional Pipe Flow," *Physics of Fluids*, Vol. 17, No. 1, 2005, p. 011706.

[30]Soueid, H., "Secondary Vortices in Turbulent Square Duct Flow: Effect of the Choice of the Cost Functional," Dipartimento di Ingegneria Ambientale, DIAM Internal Rept. 1/05, Univ. of Genoa, Genoa, Italy, Sept. 2005, available from the author upon request (soueid@diam.unige.it).

[31]Luchini, P., "Reynolds-Number-Independent Instability of the Boundary Layer over a Flat Surface: Optimal Perturbations," *Journal of Fluid Mechanics*, Vol. 404, 2000, pp. 289–309.

[32]Press, W. H., Flannery, B., Teukolsky, S. A., and Vetterling, W. T., *Numerical Recipes in Fortran*, Cambridge Univ. Press, Cambridge, England, U.K., 1992.

[33]Schmid, P. J., and Henningson, D. S., *Stability and Transition in Shear Flows*, Springer, New York, 2001.

[34]Trefethen, L. N., *Spectral Methods in MATLAB*, Society for Industrial and Applied Mathematics, Philadelphia, 2000.

[35]Gunzburger, M. D., *Perspectives in Flow Control and Optimization*, Society for Industrial and Applied Mathematics, Philadelphia, 2002.

[36]Corbett, P., and Bottaro, A., "Optimal Linear Growth in Swept Boundary Layers," *Journal of Fluid Mechanics*, Vol. 435, 2001, pp. 1–23.

A. Plotkin
Associate Editor